

22. THIN-SECTION PETROGRAPHY OF THE MEDITERRANEAN EVAPORITES

22.1. PETROGRAPHIC DATA AND COMMENTS ON THE DEPOSITIONAL ENVIRONMENT OF THE MIOCENE SULFATES AND DOLOMITES AT SITES 124, 132 AND 134, WESTERN MEDITERRANEAN SEA

Gerald M. Friedman, Department of Geology, Rensselaer Polytechnic Institute, Troy, New York

INTRODUCTION

The purpose of this study was to examine petrographically, both megascopically and in thin-section under the petrographic microscope, selected samples of evaporite rocks from DSDP boreholes in the western Mediterranean Sea (Figure 1) and to interpret the environmental conditions under which they were formed. Examination carried out in thin-section under the petrographic microscope included 33 samples; six selected samples were X-rayed to determine the presence of anhydrite, gypsum, dolomite, and calcite. In the petrographic examination, crystal fabrics were described according to Friedman (1965).

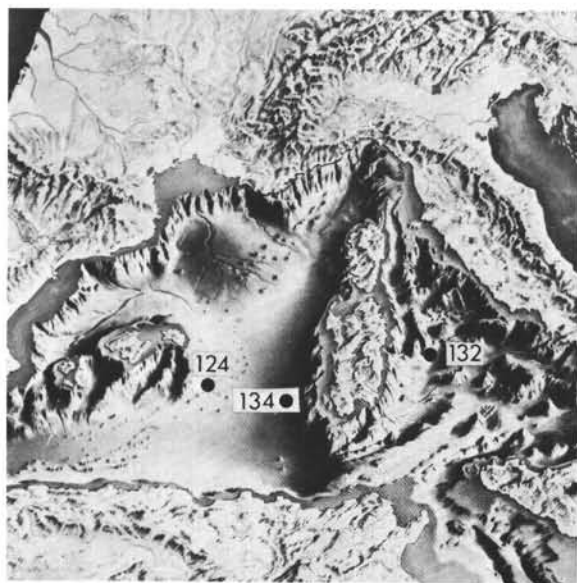


Figure 1. *Physiographic panorama of the Balearic and Tyrrhenian Basins of the western Mediterranean Sea showing the locations of the three drillsites with sequences of evaporite rocks of upper Miocene age.*

On initial examination of the rocks, it became apparent that the sedimentary structures and mineral associations are similar to those of interpreted *sabkha* deposits which I have seen in Miocene rocks of the Red Sea, in Jurassic rocks of Abu Dhabi in the Persian Gulf, in Permian rocks of west Texas, and in rocks which Shearman and Fuller (1969) have described from the Devonian of Western Canada. Since the completion of this study, and just as this paper was going to press, Hardie and Eugster (1971) presented a similar interpretation for upper Miocene evaporite rocks of Sicily.

This paper consists of two parts, the first a petrographic description of the rocks and the second an interpretation of their origin.

In the petrographic descriptions which follow, reference should be made to the cores as they appear megascopically (Figures 2 and 3). Figure 2 shows Cores 8, 9, 10, 11, 12, and 13 (to the bottom of the chicken-wire anhydrite) from Site 124; Figure 3 shows Cores 25 (Section 2), 26, and 27 from Site 132 and the upper part of Core 10 (Section 1) from Site 134.

PETROGRAPHIC DESCRIPTIONS

Site 124 – Balearic Rise

The upper part of Core 13, Section 2; all of Core 13, Section 1; Core 12; all of Core 11, Section 2; and the lower part of Core 11, Section 1; consist almost entirely of typical chicken-wire anhydrite (Figure 4). Clear, white, irregularly-shaped anhydrite nodules, up to approximately 3 cm along their long diameter, are bounded by a fine-grained, tan gray or mixed light gray and tan gray matrix.

Petrographic examination in thin-section shows the nodules to be composed of cryptocrystalline or micron-sized anhydrite crystals which increase to decimicron size near the boundaries of the nodules. Photomicrographs of similar nodules from Core 10 are discussed below. In places, small (centimicron-size) nodules of chert have formed at the expense of anhydrite. An opaque matrix, probably rich in organic matter, occupies the area between the nodules. Inter-nodular anhydrite occurs in a stellate pattern, in bundles, or in random orientation in samples in which the number of nodules is smaller and amount of matrix greater, such as in the lower part of Core 11. In this inter-nodular anhydrite, fine-grained, opaque, probably organic-rich matter is scattered between the crystals or is enclosed within them.

Massive anhydrite, above the chicken-wire anhydrite, is seen in Core 10, Section 2, of which studied samples include the intervals 74 to 76, 38 to 40, 44 to 46, and 16 to 18 cm. This anhydrite is also nodular, but the nodules are not as evident as in the chicken-wire anhydrite because they are smaller (millimeter-size), grayish white instead of clear white, and are irregularly intermixed with tannish gray anhydrite. The irregular intermixing between the grayish white and tannish gray anhydrite obscures the nodular character of this anhydrite. Moreover, these nodules are not individually bounded by a gray matrix which provides contrast to the clear white anhydrite of the underlying chicken-wire anhydrite. Most anhydrite nodules have a stellate pattern with centimicron-sized anhydrite crystals

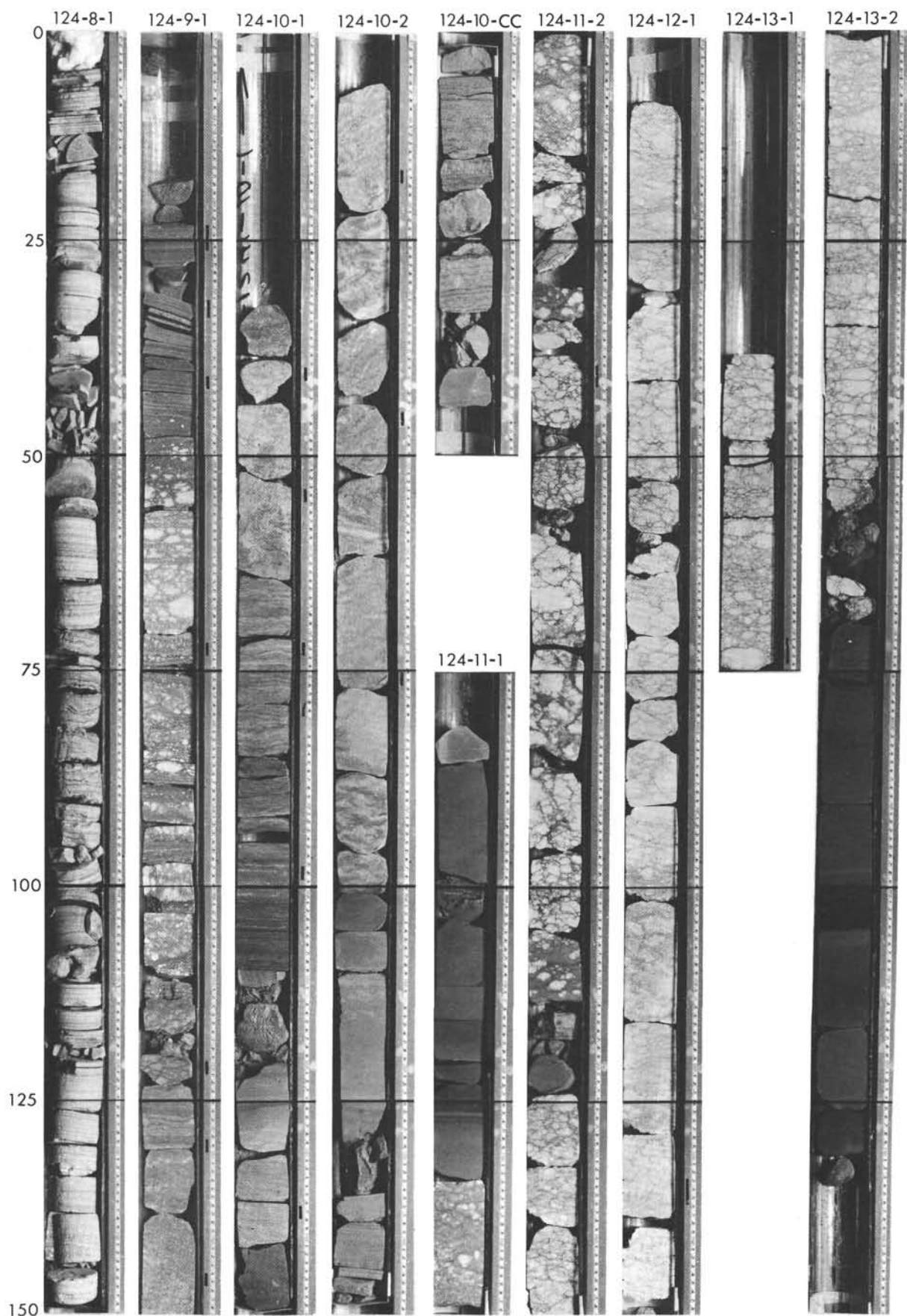


Figure 2. Photographs made shipboard of selected core sections from Site 124—Balearic Rise. The small black bars along the centimeter scales show the exact location of samples described in the text and illustrated in separate macro- and micro-photographs.

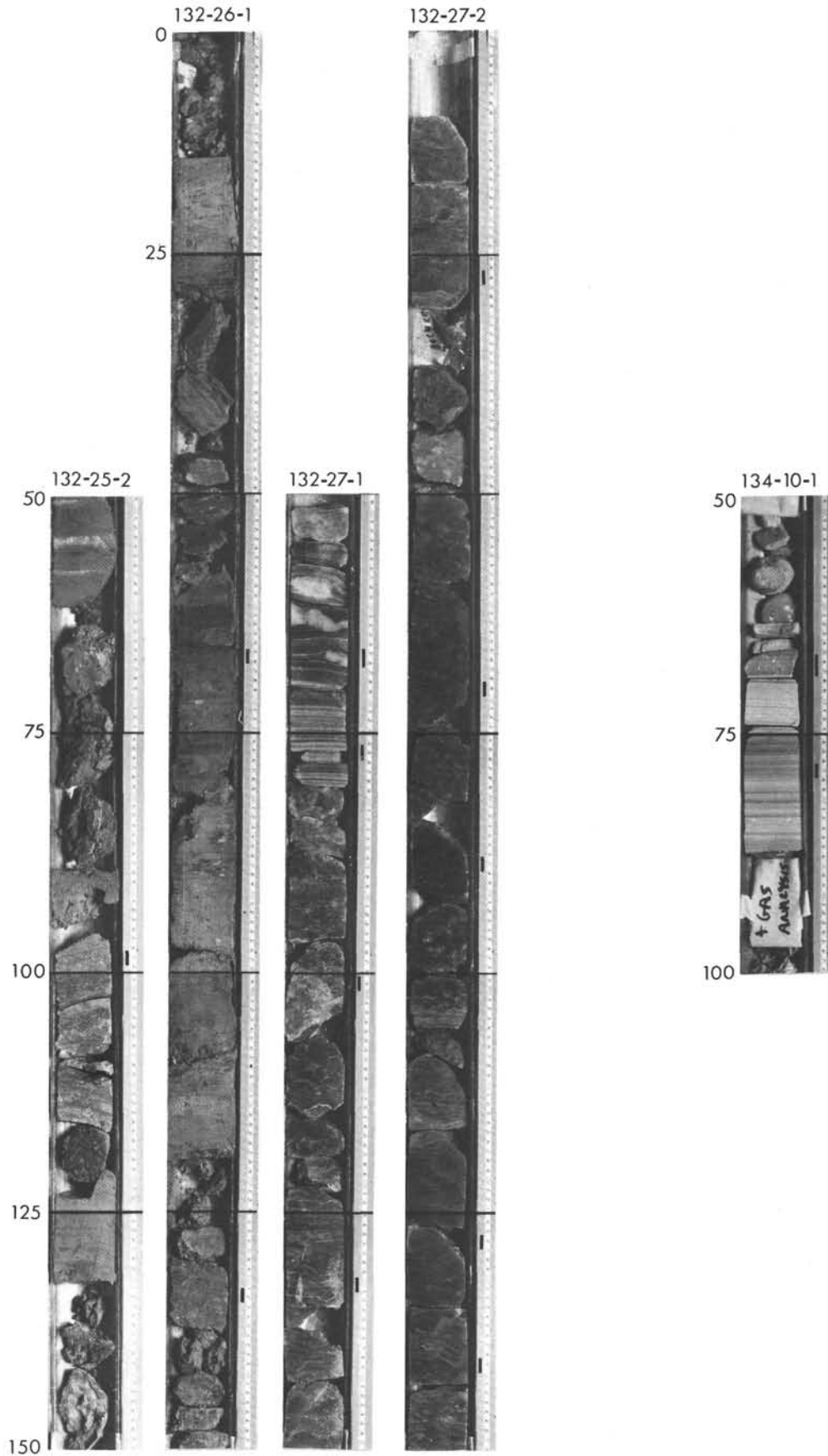


Figure 3. Selected core sections from Site 132–Tyrrenian Basin and Site 134 on the Balearic Abyssal Plain west of Sardinia. The small black bars on the centimeter scales mark the locations of samples discussed in the text and illustrated in enlargements.

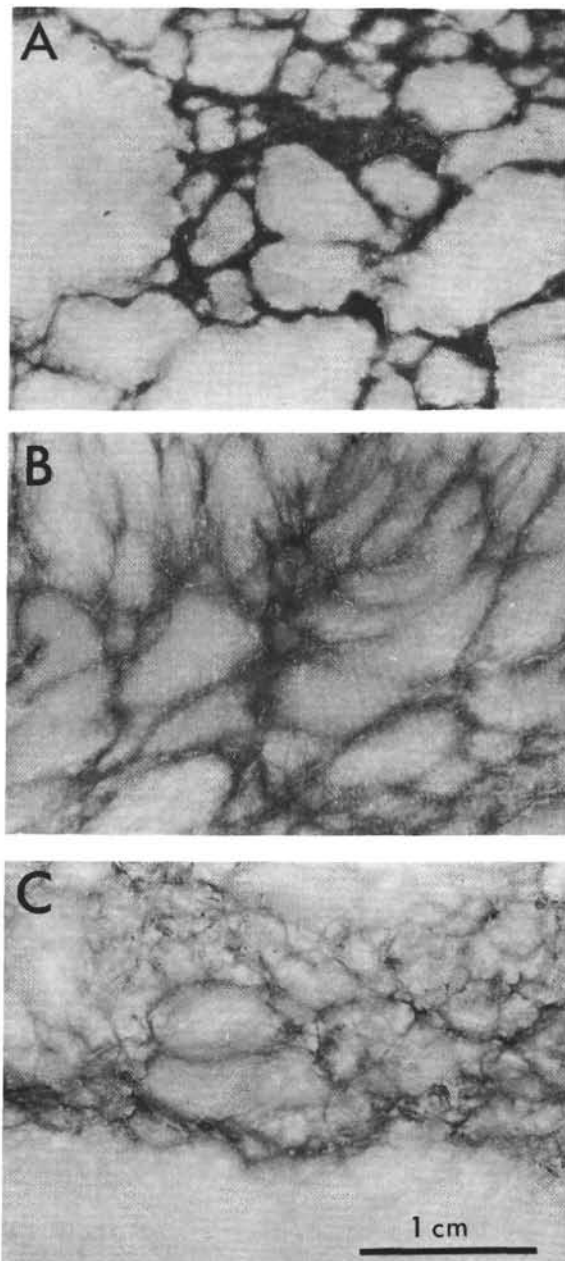


Figure 4. Nodular and chicken-wire textured anhydrite from Site 124—Balearic Rise. A = Core 11, Section 2, 39 to 42 cm; B = Core 12, Section 1, 133 to 136 cm; C = Core 13, Section 1, 71 to 73 cm.

radially arranged between the center and periphery of each nodule (Figure 5). In places, chert has replaced the anhydrite. Between the nodules, the anhydrite consists of decimicron-sized crystals which are randomly arranged, or which follow a stellate pattern, and which enclose abundant disseminated micron-sized, semi-opaque matter which is probably organic-rich. Fractures in nodules are healed with opaque material.

In Core 10, Section 1, the rocks consist mostly of anhydrite and dolomite and are, by and large, finely-laminated. The lowermost sample studied is in the interval 132 to 134 cm and is made up of dark gray dolomite (as

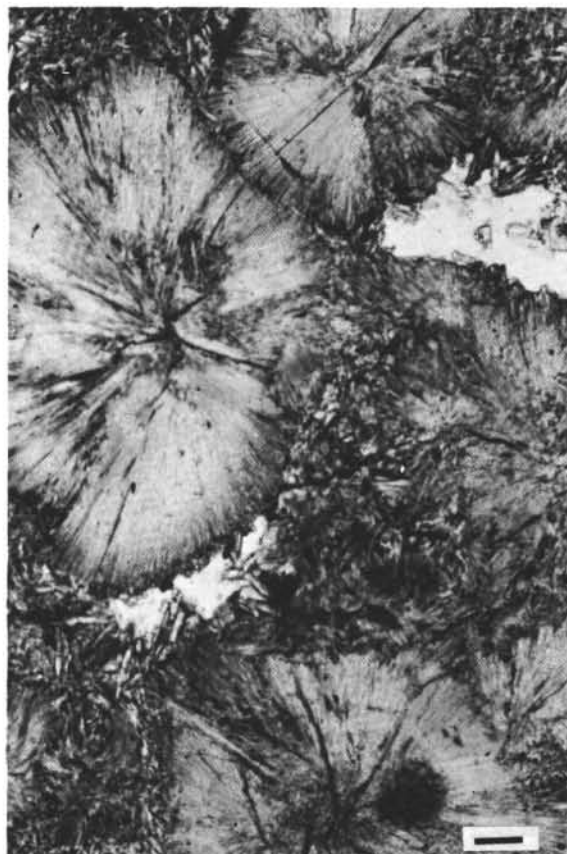


Figure 5. Anhydrite nodule with stellate arrangement of crystals. Site 124, Core 10, Section 1, Interval 53 to 55. Scale bar represents 100 microns.

identified by X-ray) with very fine laminations (Figure 6A). Under the petrographic microscope, this rock is a finely-laminated dolomicrite with micron- to decimicron-size anhydrite inclusions. Samples from the intervals 78 to 80, and 97 to 99 cm consist of finely-laminated, alternating dark and medium gray layers that are a millimeter or less in thickness and are interlaminated with grayish white anhydrite layers 3 to 4 mm thick. Under the petrographic microscope, the dark gray layers consist of semi-opaque micritic dolomite and the medium gray layers of deci- to centimicron sized anhydrite laths (Figure 7). Both layers contain micron-sized disseminated, probably organic-rich, matter. The grayish white anhydrite laminites contain only minor scattered micron-size opaque matter. The anhydrite crystals in the grayish white laminites show random to subparallel and even stellate fabrics; the crystals are variable in size and range from decimicron to centimicron. A sample from the interval 71 to 74 cm consists of undulating grayish white anhydrite laminites 2 to 4 mm thick, tannish gray anhydrite laminites 1 to 2 mm thick, and black, probably dolomitic, laminites 1/4 to 1/2 mm thick which resemble stylolites (Figure 6B). Under the petrographic microscope, the black laminites are a dark gray, semi-opaque micrite; the anhydrite consists of micron to decimicron sized crystals that are in random or sub-parallel orientation. Scattered micron sized opaque material, probably organic-rich, is scattered in between decimicron-sized anhydrite

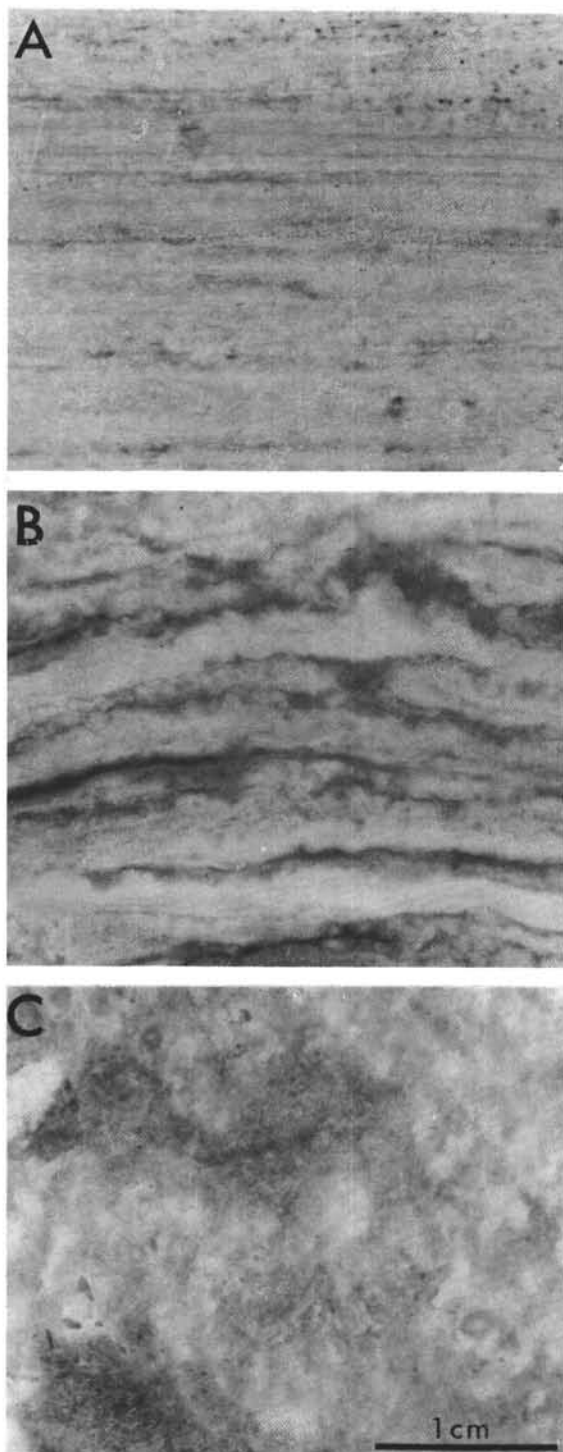


Figure 6. *Laminated and nodular textures in Core 10, Section 1 of Site 124. A = finely laminated dolomicrite at 132 to 134 cm; B = stylolites with thick grayish white laminae of anhydrite alternating with darker dolomite at 71 to 72 cm; C = nodular anhydrite impregnated with organic matter at 53 to 55 cm.*

laths. In the upper part of Core 10, Section 1, which was studied in thin-section by using samples from the intervals 53 to 55 and 39 to 41 cm, the rock consists of intermixed



Figure 7. *Couplets consisting of alternating anhydrite layers and dark gray semi-opaque, dolomite. Site 124, Core 10, Section 1, Interval 97 to 99 cm. Scale bar represents 100 microns; arrow indicates up.*

whitish gray (in part nodular) and tannish gray anhydrite (Figure 6C). Nodules of the whitish gray anhydrite display a stellate (radial) pattern (Figures 5 and 8). The tannish gray anhydrite is impregnated with semi-opaque, probably organic-rich, matter (Figure 9). Between the nodules occur randomly oriented decimicron-sized anhydrite laths (Figure 10).

Core 9 is of variable lithology. In its lower part, as represented by sample interval 143 to 146 cm, between the intermixed whitish-gray (in part nodular) and tannish gray anhydrite, occur intercalated dark gray to black laminites. Under the petrographic microscope the laminites are completely opaque and black in color and may be organic-rich (Figure 11). The whitish gray anhydrite has, in part, a stellate fabric. The contiguous overlying rock, as represented by sample interval 128 to 130 cm, consists of irregularly undulating light and dark laminites. The light-colored laminites are anhydrite, in part occurring as millimeter sized nodules, and the dark laminites which show up as black and opaque under the petrographic microscope, are probably anhydrite impregnated with organic matter. Sample interval 119 to 122 cm, only 6 cm higher in the core, shows irregularly shaped white anhydrite nodules, up to 1-1/2 cm along their long diameter, coated by dark gray to black matter, which under the microscope



Figure 8. *Anhydrite nodules with internodular lath-shaped anhydrite crystals. Site 124, Core 10, Section 1, Interval 53 to 55 cm. Scale bar represents 100 microns.*

is opaque and probably organic-rich. The anhydrite nodules consist of deci- to centimicron laths which are in a stellate pattern or are arranged in a random orientation (Figure 12). The rock above this sample interval, up to about 45 to 49 cm, has abundant nodules of anhydrite. These are particularly obvious because they are clear white in color and are coated by dark opaque, probably organic-rich, matter. Examination under the petrographic microscope of a sample from the interval 70 to 73 cm shows that the nodules consist of micron-sized to cryptocrystalline anhydrite (Figure 13). Black opaque, probably organic-rich, matter separates the nodules and encloses decimicron-sized laths of anhydrite. In the uppermost part of the core, above the nodular anhydrite, the rock consists of couplets of alternating dark gray and light gray laminites (Figure 14). These were studied in intervals 23 to 26, 31 to 33, and 40 to 42 cm. The light gray laminites tend to be about 1 to 3 mm thick, whereas the dark gray ones are 1/4 to 1/2 mm thick. The light gray laminites consist of decimicron-sized subparallel laths of anhydrite (Figure 15), and the dark gray laminites are semi-opaque to opaque under the petrographic microscope and may be in large part composed of organic matter, some of it probably micritic dolomite. Gypsum shows up on the X-ray record, but its petrographic habit under the microscope remained elusive. Centimicron-sized anhydrite nodules occur sporadically in the light gray



Figure 9. *Concentration of semi-opaque, cryptocrystalline, probably organic-rich, matter in anhydrite. Site 124, Core 10, Section 1, Interval 53 to 55 cm. Scale bar represents 100 microns.*

layers; the anhydrite in these nodules is micron-sized or cryptocrystalline. Some nodules are opaque because of the inclusion of opaque material which is probably organic-rich.

Anhydrite nodules commonly displace the laminites; clearly they have formed after the deposition of the laminites since they displace them.

Site 132 – Tyrrhenian Basin

The cores from this site differ from those of Site 124 in that gypsum is a much more common component of the rocks. This is shown in the X-ray record. Yet, the depositional fabric, such as the nodular character as seen both in hand specimen and under the petrographic microscope, indicates that the original mineral was anhydrite. Under the petrographic microscope, various replacement fabrics of the original anhydrite are apparent, and it is not always easy to determine whether anhydrite, gypsum, or both are present. Hence, in the following description of the samples studied, I will refer to calcium sulfate rather than to gypsum or anhydrite except where it is easy to distinguish between these two minerals.

In the study of cores from Site 132, selected samples were taken which were considered to be genetically important, and only these specific samples will be described. Throughout these descriptions, reference should be made to Figure 3.

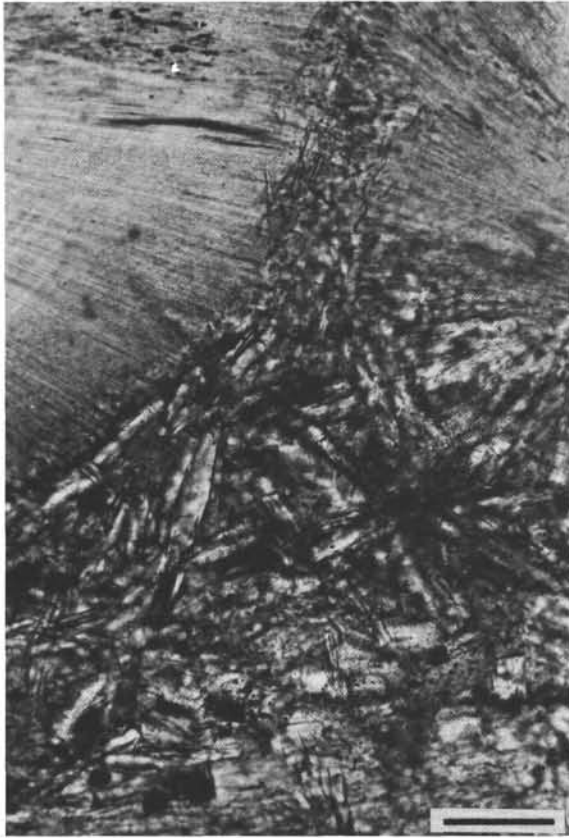


Figure 10. *Boundary between two anhydrite nodules; anhydrite laths adjacent to nodules. Site 124, Core 10, Section 1, Interval 39 to 41 cm. Scale bar represents 100 microns.*



Figure 11. *Anhydrite laths and dark, probably organic-rich in part, pelletlike material. Site 124, Core 9, Section 1, Interval 143 to 146 cm. Scale bar represents 100 microns.*

Core 25, Section 2, Interval 96-98 cm (Figure 16A):

A flat-pebble conglomerate represents this interval. Finely-laminated angular flat pebbles of brown coloration are separated by transparent porphyrotopic sulfate, mostly gypsum. Under the petrographic microscope, the porphyrotopes have been partially replaced by finely-crystalline sulfate along fractures, cleavage faces, and at random. X-ray examination of this rock shows gypsum to be the dominant mineral. The finely-laminated flat pebbles consist of micron-sized crystals of carbonate (dolomite according to the X-ray record) and are semi-opaque in thin section suggesting the abundance of organic-rich matter.

Core 26, Section 1, Interval 131-133 cm (Figure 16B):

This interval consists of variably light to medium gray finely-laminated rock in which laminites of sulfate, 4 to 6 mm thick, alternate with laminites of dark gray opaque material, 1/3 to 1 mm thick, which is probably rich in organic matter. The opaque matter also follows fractures within the rock. The sulfate consists of micron-sized crystals which have been replaced along fractures, laminations, or cleavage faces, but deci- to centimicron sized sulfate, including millimeter-sized gypsum porphyrotopes.

Core 27, Section 1, Interval 65-66 cm (Figure 16C):

A white sulfate nodule, about 1-1/2 cm in diameter, and medium gray massive sulfate are intercalated with grayish

black laminations. Under the petrographic microscope, the crystal size of the sulfate ranges between cryptocrystalline and centimicron. Several generations of sulfate replacement are observed. Poikilotopes of sulfate enclose an earlier generation of micron to decimicron sized sulfate, and coarsely-crystalline sulfate ramifies through finely-crystalline sulfate suggesting that the coarsely-crystalline sulfate has formed at the expense of finely-crystalline sulfate.

Core 27, Section 1, Intervals 98-100 cm and 129 to 131 cm:

These samples consist of light to dark gray partially mottled, more or less massive, sulfate with irregularly intercalated fine-grained dark laminites, which under the petrographic microscope are semi-opaque to opaque and probably organic-rich. The sulfate ranges in crystal size from cryptocrystalline to micron and decimicron sized. Millimeter- and even centimeter-sized gypsum has ramified through finely-crystalline sulfate indicating that the coarsely-crystalline gypsum is younger.

Core 27, Section 2, Interval 25-27 cm (Figure 17A):

Light gray to clear white irregularly-shaped sulfate nodules are interlaminated with tannish brown and light gray laminites and are in part enclosed in a grayish black



Figure 12. *Stellate anhydrite nodule, Site 124, Core 9, Section 1, Interval 119 to 122 cm. Scale bar represents 100 microns.*

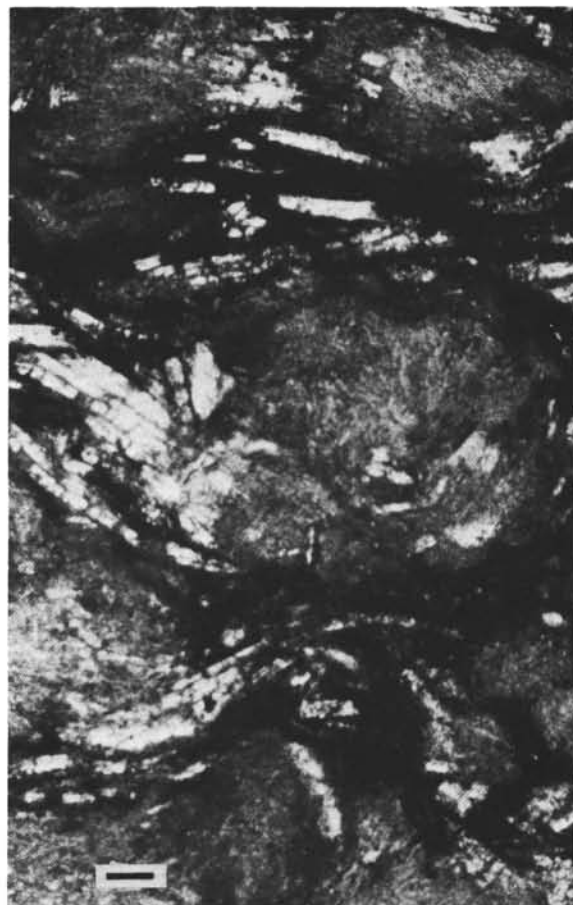


Figure 13. *Nodules consisting of cryptocrystalline anhydrite separated by dark opaque, probably organic-rich, matter enclosing anhydrite laths. Site 124, Core 9, Section 1, Interval 70 to 73 cm. Scale bar represents 100 microns.*

matrix. Pyrite crystals occur in patches. Under the petrographic microscope, the tannish brown laminites consist of carbonate pelmicrites, probably dolomite. The grayish black matrix is opaque under the petrographic microscope and may be organic-rich. The sulfate is of several generations; an example is a fabric of micron-sized sulfate crystals which ramify irregularly and randomly through large millimeter-sized crystals, hence the finely-crystalline sulfate has replaced older coarsely-crystalline sulfate.

Core 27, Section 2, Intervals 68 to 70 cm (Figure 17B) and 86 to 88 cm:

Samples contain white millimeter-sized sulfate nodules which are mostly gypsum according to the X-ray record. Many of them run into one another, giving rise to an enterolithic fabric. They are interlaminated with or bounded by a deep reddish brown material which, under the petrographic microscope in transmitted light, is completely opaque and, in reflected light, is red. This matrix is mostly limonite. X-ray examination of a sample from the interval 68 to 70 cm shows that gypsum is the dominant mineral present.

Core 27, Section 2, Interval 125 to 127 cm:

Sulfate nodules, almost 2 cm along the long diameter, are set in an undulating finely-laminated matrix of alternating light gray and tannish brown laminites. Petrographic microscope examination shows that the light gray laminites are sulfate and the tannish brown laminates are opaque, probably organic-rich material. The sulfate crystals consist of poikilotopes that have been largely replaced by a (younger) micron-sized sulfate fabric.

Core 27, Section 2, Interval 138 to 140 cm (Figure 17C):

Sulfate nodules, one half to one centimeter in diameter, are bounded by dark gray opaque, probably organic-rich, material. Poikilotopes of anhydrite have been mostly replaced by a micron sized sulfate fabric.

Site 134 – Balearic Abyssal Plain

Petrographic study of material from cores of this site included the examination of only two samples. Both of these were taken from Section 1 (see Figure 3). They are described below.

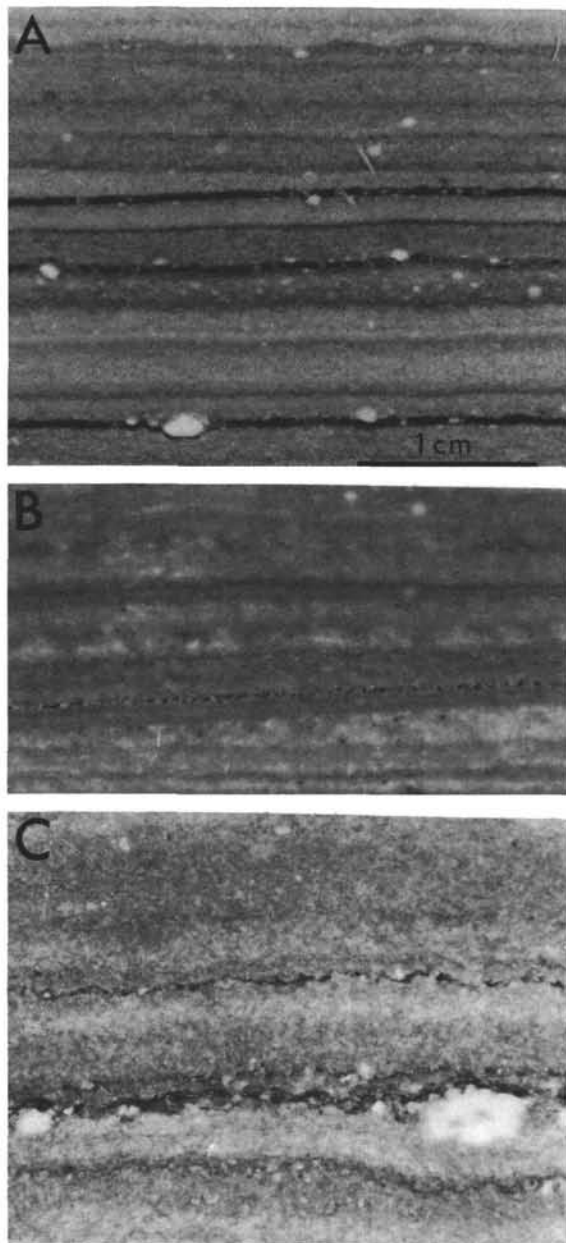


Figure 14. *Couplets of alternating dark gray and light gray laminites in Core 9, Section 1 of Site 124. A = 23 to 26 cm; B = 31 to 33 cm; C = 40 to 42 cm. Figure 15 is a microphotograph of the interval illustrated in C. The white nodules are pure anhydrite.*

Core 10, Section 1, Interval 65 to 68 cm (Figure 18):

This interval consists of finely and regularly interlaminated grayish black and light gray laminites. The grayish black laminites are 1/2 mm thick, whereas the light gray laminites are 2 to 3 mm thick. Examination under the petrographic microscope shows the grayish black laminites to consist of opaque, probably organic-rich, matter; the light gray laminites are composed of anhydrite. Set between the laminites are white nodules of anhydrite a fraction to 3 or 4 mm in diameter. These nodules appear as a diffuse gray



Figure 15. *Anhydrite laths in subparallel orientation. Site 124, Core 9, Section 1, Interval 40 to 42 cm. Scale bar represents 100 microns.*

under plane-polarized light; the surrounding matrix between these nodules consists of decimicron-sized anhydrite laths.

Core 10, Section 1, Interval 76 to 78 cm:

This interval consists of finely and regularly interlaminated dark gray and grayish white laminites. Of these, the grayish white laminites are more abundant. Anhydrite nodules are not apparent. The thin-section of this rock shows the laminites to consist mostly of micrite (micron-sized crystals), probably anhydrite, with abundant finely-disseminated opaque inclusions. This makes the laminites semi-opaque. Decimicron-sized anhydrite laths are interspersed within the micritic, semi-opaque matrix.

ORIGIN OF THE ROCKS

The nodular anhydrite, particularly with the typical "chicken-wire lattice structure" that is so evident at Site 124, in Cores 11, 12, and 13, is indicative of subaerial exposure of soft sediments in which the nodules are formed by displacement of the host sediment. This inference was arrived at by Murray (1964) from examination of subsurface evaporites even before the widespread study of modern anhydrite of the Persian Gulf. Withington (1961) was probably the first to suggest, as a general mechanism, the precipitation of anhydrite as nodules from interstitial brines.

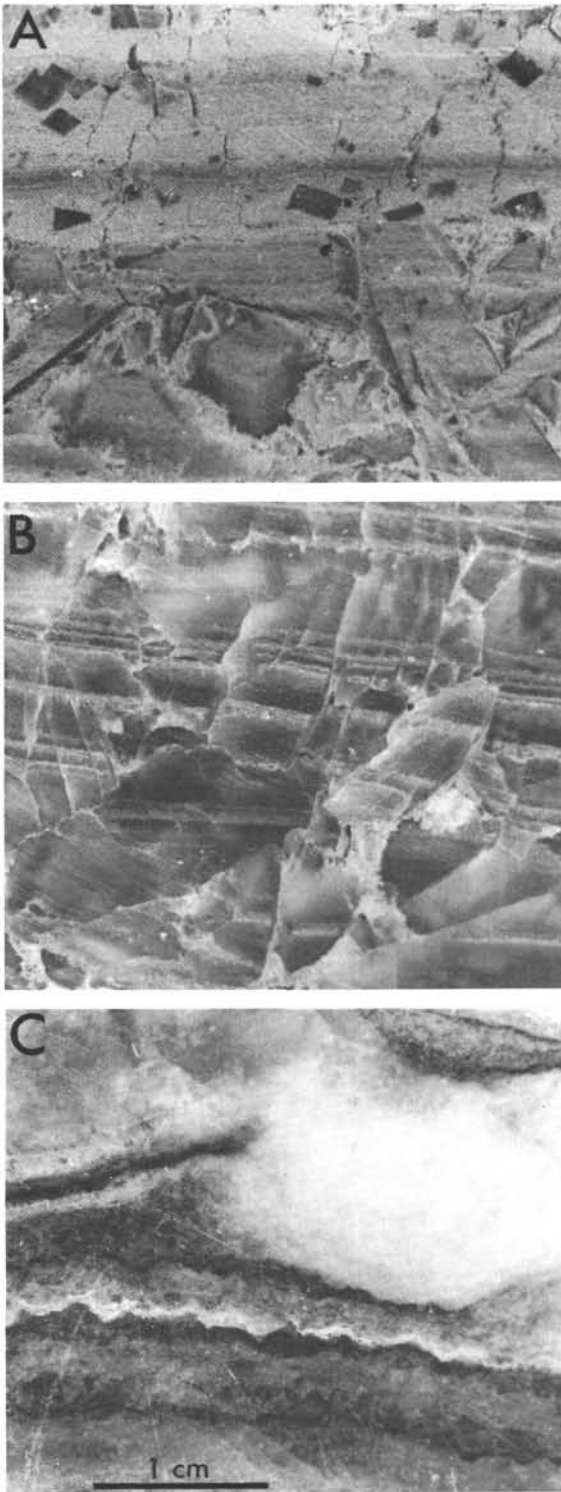


Figure 16. *Recrystallized gypsum in Site 132 in the Tyrrhenian Basin. A = flat-pebble conglomerate from Core 25, Section 2 at 96 to 98 cm; B = secondary gypsum (fractured) replacement of former laminated anhydrite from Core 26, Section 1 at 131 to 134 cm; C = white sulfate nodule showing several generations of replacement from Core 27, Section 1 at 64 to 67 cm.*

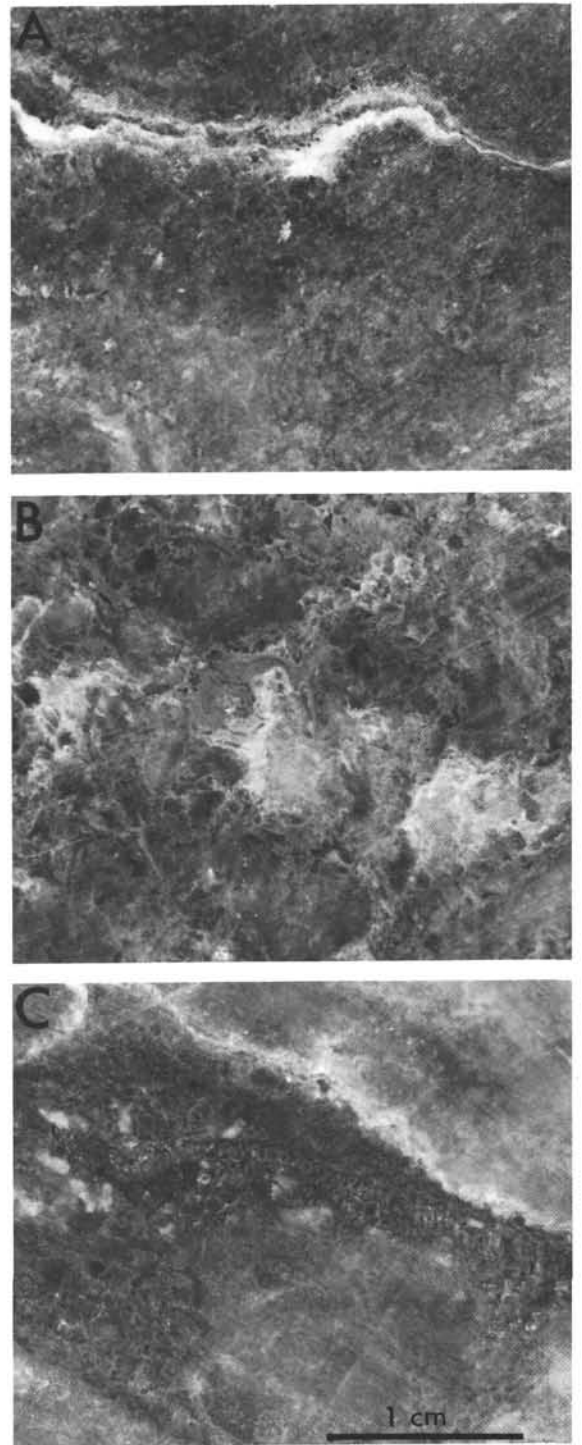


Figure 17. *Irregular shaped nodular growth of sulfate minerals from Core 27, Section 2 at Site 132-Tyrrhenian Basin. A = tannish-brown and light gray laminates at 23 to 26 cm; B = entrolithic fabric interlaminated with a deep reddish brown material and limonite matrix at 66 to 69 cm; C = large nodules of former anhydrite now completely replaced by gypsum at 138 to 141 cm.*

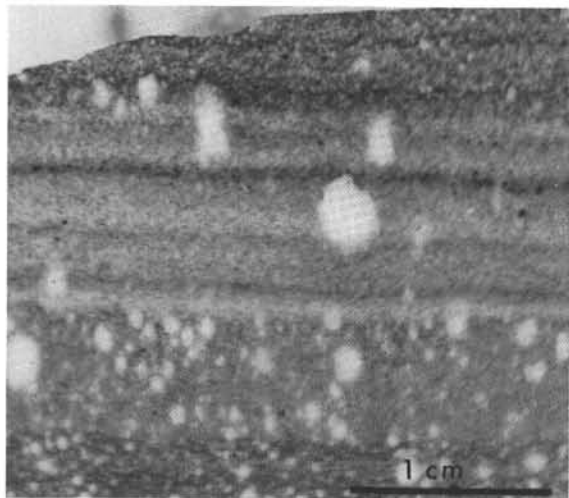


Figure 18. Laminated anhydrite with scattered nodules from Site 134—Balearic Abyssal Plain. This interval is from Core 10, Section 1, 65 to 67 cm.

With the discovery of modern anhydrite nodules in the Persian Gulf (Figure 19), comparable to those found in the rock record, the interpretation has become generally accepted that nodular anhydrite is an indicator of subaerial origin in tidal flats of arid regions, generally known as *sabkhas* (Friedman and Sanders, 1967; Holliday, 1968; Kinsman, 1966, 1969; Kendall and Skipwith, 1969; Shearman, 1966; Shearman and Fuller, 1969; West, Brandon and Smith, 1968; others). In the *sabkha* environment, anhydrite nodules form in carbonate sediments of the capillary zone above the groundwater table. In this sediment the multicrystalline anhydrite nodules grow by physical displacement. The mechanical force of crystal growth, exerted by the anhydrite crystals growing in a nodule, displaces the surrounding sediment. Hence, laminae of the host sediment become physically displaced and bend around the nodules. This is evident, not only in the modern environment, but also in the Miocene cores of the Mediterranean (see, for instance, Figure 2, Site 124, Core 9, Section 1 at various places; particularly evident under the microscope). Continuing growth of nodules in the host sediment leads to a fabric where nodules merge into one another, hence, continuous layers may really be compound aggregates of nodules. These compound nodular aggregates may take on most irregular shape and as a result of this continuing growth form enterolithic structures (Shearman, 1966). The term *enterolithic* means literally “like a stony intestine” and describes the appearance of the structures in side view (Shearman and Fuller, 1969; also see Figure 3, Site 132, Core 27, Section 1, Interval 60 to 63 cm).

As the nodules grow and coalesce, their original boundaries become distorted and the thin contorted layers which surround them no longer form complete envelopes. The resulting texture has been termed *penemosaic* (Rooney and French, 1968). Holliday (1969) has shown that anhydrite with typical nodular texture passes laterally into anhydrite with penemosaic texture. As a result of the early diagenetic changes within the host sediment of the capillary

zone in the *sabkha*, a wide variety of textures can form which are derived from the incipient nodular texture.

Observations in the *sabkhas* of the Persian Gulf show that, because of their platy crystal habit and natural moisture content, the nodules in the capillary zone are soft and putty-like and easily deformed. With progressive compaction, depending on rigidity and drainage characteristics of the host sediment, anhydrite nodules progressively become flattened and ultimately laminar (Shearman and Fuller, 1969). Hence all transitional stages exist between nodular and laminar anhydrites. Shearman and Fuller (1969) demonstrate how laminar anhydrite had originally grown as anhydrite nodules in the host sediment. Although no conclusive evidence exists at present for the Miocene rocks of this study, it has been shown that laminated anhydrite may not be a sedimented deposit, but an early diagenetic emplacement within a preexisting host (Shearman and Fuller, 1969).

Evidence for the conditions under which the Miocene rocks were deposited is provided by other comparisons with modern *sabkha* sediments. These include the presence of fine laminae, dolomite and flat-pebble conglomerate (see Figure 3, Site 132, Core 25, Section 2, Interval 96 to 98 cm) and the absence or dearth of fossils (Braun and Friedman, 1969; Friedman, 1969; Friedman and Sanders, 1967; Laporte, 1967; Matter, 1967; Schenk, 1967; Shinn, Ginsburg and Lloyd, 1965; Textoris and Carozzi, 1966). In the Persian Gulf, the laminated sediment within which the anhydrite nodules grow consists of blue green algal mats. The mats act as sediment traps for lime mud which subsequently becomes dolomitized. Along the Red Sea coast, algal mats secrete laminites (Figure 20; Friedman and others, manuscript) that by and large consist of high-magnesian calcite. The mats preferentially concentrate magnesium in the organic substance. The total magnesium concentration between the organic matter and the high-magnesian calcite exceeds that required for dolomitization (Friedman and others, manuscript). Hence, finely-laminated dolomites are a diagnostic feature of tidal (*sabkha*) sediments. The fine laminae of the Miocene rocks studied, particularly in Cores 8 and 9 and in Core 10, Section 1, at DSDP Site 124 (Figure 2), are of the kind now interpreted as algal stromatolites (Braun and Friedman, 1969; Friedman, 1969; Friedman and Sanders, 1967; La Porte, 1967; Matter, 1967; Schenk, 1967; Shinn, Ginsburg and Lloyd, 1965; Textoris and Carozzi, 1966; others). The semi-opaque to opaque character of alternate laminae, as shown under the petrographic microscope, suggests that these laminae are or were rich in organic matter. This is in keeping with the concept of derivation from algal mats. Where nodules are abundant, the original mats have become distorted, even broken, and the organic matter has become scattered among the anhydrite crystals. This was a common observation in the Miocene rocks studied. How much of the organic matter has been removed by oxidation and/or replacement by anhydrite or dolomite in the rocks studied needs to be investigated. The anhydrite and dolomite together with the opaque, organic-rich matter have preserved the original outlines of the algal mats. Anhydrite layers replace the algal mats parallel to the laminae; replacement appears to have been guided along planes

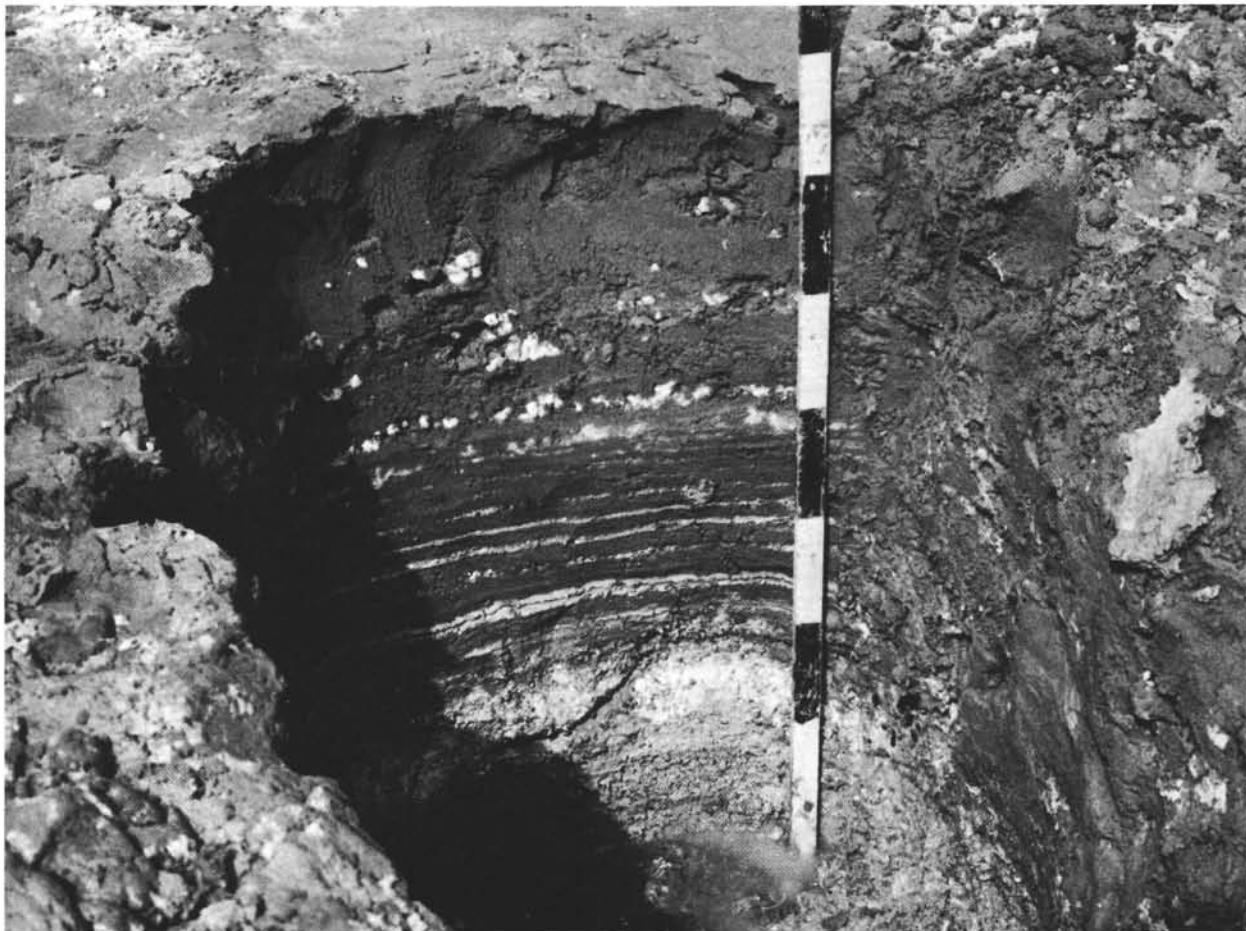


Figure 19. Sample pit in sabkha sediments of Abu Dhabi, Persian Gulf. Horizontal layers are those of buried algal mats; nodules and white laminae consist of anhydrite. Anhydrite nodules have grown in a mixture of carbonate and terrigenous sediment.

between the mats. The greater abundance of anhydrite than dolomite suggests that anhydrite has replaced dolomite laminae; a common observation in *sabkha*-derived evaporites (Rooney and French, 1968; Lambo, 1964). The presence of anhydrite nodules in the fine laminae (an association which is diagnostic of *sabkha* sediments) negates the possibility that the laminae may be annual precipitates such as those interpreted as varves in basinal deposits.

Another rock which shows the diagnostic characteristics of tidal-flat origin is the flat-pebble conglomerate (Figure 16A). Flat-pebble conglomerates form on tidal flats during desiccation. Drying results in mud cracks from which the chips subsequently spall. These chips are concentrated during the next flooding (Shinn, 1968; Braun and Friedman, 1969).

The Miocene rocks studied are devoid of fossil fragments; the hypersaline environment of the *sabkha* does not support a living fauna, other than algal mats.

The presence of halite at Site 134, Core 8, with its included anhydrite nodules and fine laminae, is in line with Shearman's (1966) interpretation that "Few, if any, of the soluble salts appear to be present as primary precipitates; instead, their fabrics testify to complex series of replacements, all of which tend to lead back to anhydrite and gypsum" (p. B 214).

A comparison of the cores studied from Site 134 with those from Site 132 shows that in the rocks at Site 132 much of the original anhydrite has been replaced by gypsum. This observation is intriguing. Gypsum in the subsurface transforms to anhydrite, and near-surface anhydrite transforms to gypsum; the depth of the hydration is generally less than 1,000 feet (Kinsman, 1966). Yet, the cores from both sites sampled the Miocene evaporites at very similar depths. Hence, the explanation for the replacement of anhydrite by gypsum at Site 132 must be found elsewhere. Shearman (1966) noted that throughout large areas of the inland part of the *sabkhas* of the Persian Gulf the anhydrite passes laterally into gypsum; often by transition. Field evidence suggests that these gypsum crystals are the result of hydration of anhydrite caused by the influx of less saline groundwaters from the country rock inland of the *sabkhas*. That this explanation is likely is suggested by the presence of abundant limonite between the gypsum crystals in several of the samples studied (Figure 17B). In fact, the core containing abundant gypsum is the same one in which limonite is a prominent constituent between the sulfate layers. Hence, the explanation is offered that parts of the cores at Site 132 represent a terminal environment of an inland part of the *sabkha* in which less saline groundwaters were active.

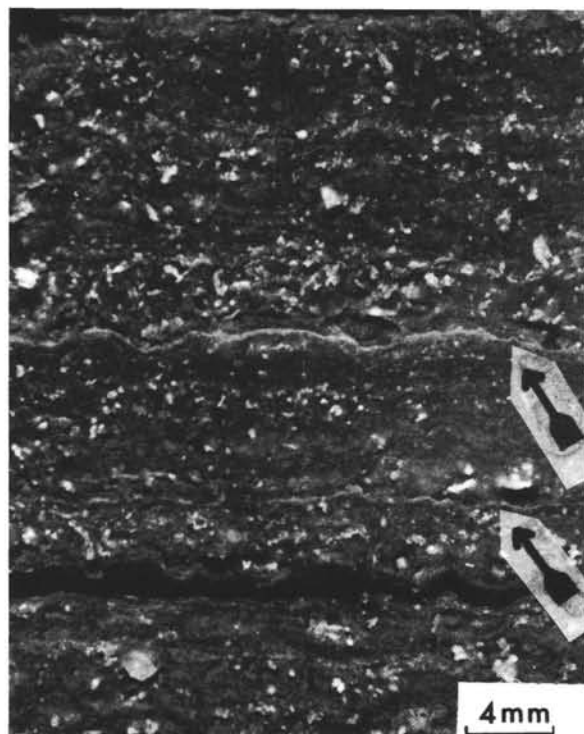


Figure 20. Core through algal mats of hypersaline pool along Red Sea coast. Most of the core material consists of laminated organic matter of the algae. Between the mushy organic laminae are laminae consisting of high-magnesian calcite (see arrows).

The evidence is that, during formation of the rocks studied, the areas of what is now the Mediterranean Sea at Sites 124, 132, and 134 almost completely lacked a cover of water. Instead, these areas largely consisted of emergent, brine-logged flats.

CONCLUSIONS

A petrographic study of the evaporite rocks in cores obtained from Sites 124, 132, and 134 suggests that these rocks originated in a subaerial *sabkha* environment. Thus, what is today a part of the floor of the Mediterranean Sea was, during the times represented by these rocks, nearly devoid of water cover and consisted of emergent brine-logged flats.

ACKNOWLEDGMENTS

I wish to thank R. J. Fiske for the sampling of the cores. The project was initiated at the suggestion of William B. F. Ryan who with the assistance of B. C. Schreiber supplied the macrophotographs of the polished core sections. The cost of the thin-sectioning and microphotography was underwritten by the Deep Sea Drilling Project, through arrangements made by N. T. Edgar.

REFERENCES

Braun, M. and Friedman, G. M., 1969. Carbonate lithofacies and environments of the Tribes Hill Formation (Lower Ordovician) of the Mohawk Valley, New York. *J. Sediment. Petrol.* **39**, 113.

- Friedman, G. M., 1965. Terminology of crystallization textures and fabrics in sedimentary rocks. *J. Sediment. Petrol.* **35**, 643.
- , 1969. Recognizing tidal environments in carbonate rocks with particular reference to those of the lower Paleozoics in the Northern Appalachians. *Geological Society of America, Northeastern Section Fourth Annual Meeting, Abstracts with Programs for 1969*. Part 1, 20.
- Friedman, G. M. and Sanders, J. E., 1967. Origin and occurrence of dolostones. In Chilingar, G. V., Bissell, H. J., and Fairbridge, R. W., 1967, *Developments in Sedimentology, 9a, Carbonate rocks*. Elsevier, Amsterdam, 471 p.
- Friedman, G. M., Amiel, A. J., Braun, M., and Miller, D. S. Manuscript, Algal mats, carbonate laminites, ooids, oncolites and pellets in sea-marginal hypersaline pool, Gulf of Agaba (Elat), Red Sea.
- Hardie, J. L. and Eugster, H. P., 1971. The depositional environment of marine evaporites: a case for shallow, clastic accumulation. *Sedimentology*. **16**, 187.
- Holliday, D. W., 1968. Early diagenesis in Middle Carboniferous nodular anhydrite of Spitsbergen. *Yorkshire Geol. Soc. Proc.* **36**, 277.
- , 1969. The origin of penemosaic texture in evaporites of the Detroit River formation (Middle Devonian) in Northern Indiana: Discussion of a paper by L. F. Rooney and R. R. French. *J. Sediment. Petrol.* **39**, 1256.
- Kendall, C. G. St. C. and Skipwith, Sir P. A. D'E., 1969. Holocene shallow-water carbonate and evaporite sediments of Khor al Bazam, Abu Dhabi, Southwest Persian Gulf. *Bull. Am. Assoc. Petrol. Geologists*. **53**, 841.
- Kinsman, D. J. J., 1966. Gypsum and anhydrite of Recent age, Trucial Coast, Persian Gulf. In Raup, J. L., ed., *Second Symposium on Salt, Northern Ohio Geol. Soc. Cleveland*. **1**, 302.
- , 1969. Modes of formation, sedimentary associations, and diagnostic features of shallow-water and supratidal evaporites. *Bull. Am. Assoc. Petrol. Geologists*. **53**, 830.
- Lambo, W. A., 1964. Geology of the Silver Plains gypsum deposit. Master's Thesis, University of Manitoba, 91 p.
- LaPorte, L. F., 1967. Carbonate deposition near mean sea-level and resultant facies mosaic: Manlius Formation (Lower Devonian) of New York State. *Bull. Am. Assoc. Petrol. Geologists*. **51**, 73.
- Matter, Albert, 1967. Tidal flat deposits in the Ordovician of Western Maryland. *J. Sediment. Petrol.* **37**, 601.
- Murray, R. C., 1964. Origin and diagenesis of gypsum and anhydrite. *J. Sediment. Petrol.* **34**, 512.
- Rooney, L. F. and French, R. R., 1968. Allogenic quartz and the origin of penemosaic texture in evaporites of the Detroit River Formation (Middle Devonian) in Northern Indiana. *J. Sediment. Petrol.* **38**, 755.
- Schenck, P. E., 1967. The Macumber Formation of the Maritime Provinces, Canada. A Mississippian analogue to Recent strand-line Carbonates of the Persian Gulf. *J. Sediment. Petrol.* **37**, 365.
- Shearman, D. J., 1966. Origin of marine evaporites by diagenesis. *Inst. Mining Metallurgy Trans.* **75**, 208.
- Shearman, D. J. and Fuller, J. G., 1969. Anhydrite diagenesis, calcitization, and organic laminites, Winnipegosis Formation, Middle Devonian, Saskatchewan. *Bull. Canadian Petroleum Geology*. **17**, 496.
- Shinn, E. A., 1968. Selective dolomitization of Recent sedimentary structures. *J. Sediment. Petrol.* **38**, 612.

Shinn, E. A., Ginsburg, R. N. and Lloyd, R. M., 1965. Recent supratidal dolomite from Andros Island, Bahamas. In Pray, L. C. and Murray, R. C., Dolomitization and limestone diagenesis, a symposium. *Soc. Econ. Paleontologists and Mineralogists*, Spec. Pub. 13, 180 p.

Textoris, D. A. and Carozzi, A. V., 1966. Petrography of a Cayugan (Silurian) stromatolite mount and associated

facies, Ohio. *Bull. Am. Assoc. Petrol. Geologists*. 50, 1375.

West, I. M., Brandon, A. and Smith, M., 1968. A tidal flat evaporitic facies in the Visean of Ireland. *J. Sediment. Petrol.* 38, 1079.

Withington, C. F., 1961. Origin of mottled structure in bedded calcium sulfate. *U. S. Geol. Survey Prof. Paper* 424-D, 342.

22.2. PETROGRAPHY OF A HALITE SAMPLE FROM HOLE 134 – BALEARIC ABYSSAL PLAIN

K. J. Hsü, Geologisches Institut, Eidg. Technische Hochschule, Zurich, Switzerland

William B. F. Ryan, Lamont-Doherty Geological Observatory of Columbia University, Palisades, New York
and

B. C. Schreiber, Department of Geology, Rensselaer Polytechnic Institute, Troy, New York

INTRODUCTION

Rock salt, belonging to the late Miocene evaporite series, was encountered at 344 meters below the sea floor of the Balearic Abyssal Plain west of Sardinia. A polished specimen from Section 2 of Core 10 of Hole 134¹ is illustrated in Figure 1. The lower half of the exposed face has been made into a thin-section, 4 cm × 6 cm in area.

The geological setting of Hole 134 and a description of the drill cores can be found in Chapter 15, Part I, this volume. The salt layer correlates with the subbottom M-Reflectors, which in turn can be traced directly westward to a zone exhibiting numerous diapirs in the central Balearic Basin.

The recovered salt contains layered halite intercalated with strata rich in detrital sand and silt and peppered with small irregular anhydrite nodules. In Core 8, in particular, the halite contains very thin dark laminae rich in carbonaceous material and pyrite. As yet, the organic matter has not been identified, though there is a distinct petroleum odor at these levels when cut into, and gasoline range hydrocarbons were detected in interbedded plastic oozes within the halite in Core 10, Section 1 (see Chapter 32).

THE HALITE MINERALOGY

The translucent layered halite of Figure 1 includes two distinct types of crystals. The cloudy strata (illustrated with the letter "a" on the sliced specimen) are characterized by rectangularly shaped zones of minute liquid inclusions as typified by "a" in Figure 2, and by large pyramid shaped hopper crystals. This kind of crystal structure has been

carefully documented by Dellwig (1955) and has been recognized for a long time in the manufacturing of granier salt (Badger and Baker, 1928). Quoting from Dellwig (1955, p. 89), "crystal growth is brought about by evaporation temperatures below the boiling point in order to prevent turbulence and to permit the formation of a thin surface film of high-density brine. In this film the halite crystals begin to grow. As growth continues the cube tends to sink under its own weight, although its position at the surface is maintained by surface tension. Because only one face of the cube is in contact with the high density film, growth takes place only along its edges. In this manner, while the crystal sinks, growth continues upward and outward along these edges resulting in the hollow pyramid with the apex pointing downward When the surface is disturbed, the crystals are broken or swamped and sink. The crystals are extremely delicate and can withstand very little handling. Occasionally, a number of crystals in a small area will become attached to one another to form a crust or mat which will eventually sink as a unit."

The crystal form of the euhedral crystals (the dark dusty texture in Figure 2) is outlined only by the presence of abundant liquid inclusions (of brine) in the form of negative crystals (Dellwig, 1955). As shown in the thin-section photomicrography, the euhedral crystals are sometimes fragmented and partly dissolved. They are surrounded by a clear rim ("b" in Figure 2) of varying width which is also of halite. Studies of modern playas have revealed that the clear anhedral variety of halite is a diagenetic cement and tends to replace euhedral precipitates (D. Shearman, 1970). In advanced stages of replacement, the crystal would be rid of inclusions, except for perhaps a small "dusty" relic in the center.

The clear anhedral crystals range from 50 to 300 microns in size. They comprise individual layers or bands within the halite deposit. Such interlamination of the "dusty" ("a") and clear ("d") crystals is very conspicuous

¹Site 134 – Latitude: 39° 11.84'N; Longitude: 7° 17.96'E; water depth 2664 meters. Core 10 was cut from 359 to 364 meters subbottom.